Determining upper and lower bounds for steady state strain rate during a creep test on a salt sample

Hakim Gharbi, Pierre Berest, Laura Blanco Martín, Benoît Brouard

TECHNICAL NOTE

Determining upper and lower bounds for steady state strain rate during a creep test on a salt sample

Hakim Gharbi[a], Pierre Bérest[a], Laura Blanco-Martín[b], Benoît Brouard[c]

[a]LMS, Ecole Polytechnique, IP Paris, 91 128 Palaiseau, France

[b]Mines ParisTech, Department of Geosciences, PSL Research University, 35 rue Saint Honoré, 77300 Fontainebleau, France

[c]Brouard Consulting, Paris, France

Corresponding author: Pierre Bérest, berest@lms.polytechnique.fr

Abstract

A creep test performed on a Landes salt sample during one year and a half is described. During the first year, a 0.6 MPa axial load is applied to the sample. At the end of this one-year phase, strain rate $(9\times10^{-12}\,\mathrm{s}^{-1})$ is much faster than the strain rate extrapolated from high-stress tests. Steady state strain rate is not reached. In an attempt to reach steady state strain rate "from below", a 0.9 MPa load is applied during two days before restoring the initial load (0.6 MPa). After the load is restored, reverse creep is observed first (strain rate sign changes before vanishing to zero after a few hours). Then, strain rate increases to reach $5\times10^{-12}\,\mathrm{s}^{-1}$ after five months, slower than the strain rate before the load change. Commonly accepted constitutive laws can explain this effect, which provides a lower and an upper bound for steady state strain rate. This note presents a method to determine such bounds.

Keywords

Salt creep, Steady state creep rate, Transient creep rate, Reverse creep, Very slow creep tests

1. Introduction

Many rocks, among which salt, potash or clay, are creep-prone. When submitted to a constant deviatoric stress (a non-zero shear stress; the equivalent von Mises deviatoric stress is $\sigma = \sqrt{3J_2}$, where J_2 is the second invariant of the Cauchy stress tensor), they experience time-dependent deformation. This can be observed at the laboratory: a cylindrical sample is submitted to a constant axial stress and a constant confining pressure. The difference between these two stresses is the deviatoric stress. The axial (and circumferential) strains are recorded as a function of time. In most cases, the initial strain rate is high and slowly decreases with time, see Fig. 1 (in the following, compressive stresses and contractive strains are positive; when this convention is adopted, during a uniaxial compressive test, the axial stress equals the deviatoric stress). Two questions are important both from a theoretical and a practical point of view: is there a deviatoric stress (a threshold) below which no strain rate is observed?, and does the strain rate reach an asymptotic non-zero value (steady state)?

Regarding the first question, consider the strain versus time curve recorded during a 7-month long test performed on an Avery Island salt sample (Fig. 1). The applied load is 0.2 MPa. The figure shows that creep exists – during a uniaxial test - even for this small stress deviator (rock salt uniaxial compressive strength is 25 MPa, typically). The last question is difficult to answer as well. Consider again Fig. 1a; it may seem reasonable to draw the line tangent to the last point of the curve (in mid-February 2016). The difference between the curve and its tangent is so small that one could be tempted to conclude that steady state is reached at the end of test. However, when the strain rate is computed (it is averaged on a 15-day long span to erase unavoidable fluctuations, see Fig. 1b), it is clear that a steady state strain rate has not been reached. In fact, from a mathematical point of view, when, during a time interval $0 < \tau < t$, a function is positive and monotonously decreasing, (see Fig. 1b, $\dot{\varepsilon}(\tau) > 0,\ \ddot{\varepsilon}(t) < 0$), it is impossible to predict whether its asymptotic value is zero or any strictly positive value. In addition, from an experimental point of view, this is especially difficult when the strain rates are small. In the example above, in February 2015, the strain rate is $\dot{\varepsilon} = 10^{-11}\mathrm{s}^{-1}$, approximately. The thermal expansion coefficient of salt is $\alpha_{th} = 4\times10^{-5}/^{\circ}\mathrm{C}$. When, after a δt = one-month long period, room temperature has changed by $\delta T = 1^{\circ}\mathrm{C}$, a fluctuation which is difficult to avoid at the laboratory, the strain due to thermal expansion is $\alpha_{th}\delta T = 4\times10^{-5}$, generating an apparent strain rate of $\alpha_{th}\delta T/\delta t = 1.5\times10^{-11}\,\mathrm{s}^{-1}$ – larger than the actual strain rate due to creep. In this paper, we suggest a method (based on Wawersik and Preece[2]) which allows assessing upper and lower bounds for the steady state strain rate of a sample subjected to a constant load.

2. A typical viscoplastic constitutive law

Consider the test described in Fig. 2. The applied load is σ. It is often accepted that the observed axial strain rate is the sum of a thermoelastic strain rate and a viscoplastic strain rate which, in some models, is split into a steady state strain rate and a transient strain rate

$$\dot{\varepsilon}(t) = \dot{\varepsilon}_{el} - \alpha_{th}\dot{T} + \dot{\varepsilon}_{vp} \quad \text{and in some models} \quad \dot{\varepsilon}_{vp} = \dot{\varepsilon}_s + \dot{\varepsilon}_t \tag{1}$$

where $\dot{\varepsilon}_{el} = \dot{\sigma}/E$, $\dot{\varepsilon}_s = A(T)\sigma^n$ and $\varepsilon_t(\sigma,T,t)$ satisfies a differential equation such that, when the applied stress σ is constant, $\varepsilon_t(\sigma,T,t)$ tends toward a constant value, $\varepsilon_t^*(\sigma,T)$. For instance, Munson and Dawson[3] suggested that $\varepsilon_t^*(\sigma,T)$ can be reached from above or from below, according to

$$\begin{cases} \dot{\varepsilon}_t = \left(F-1\right)\dot{\varepsilon}_s \\ F = \exp\left[\Delta\left(1-\varepsilon_t/\varepsilon_t^*\right)^2\right] \text{ when } \varepsilon_t < \varepsilon_t^* \\ F = \exp\left[-\delta\left(1-\varepsilon_t/\varepsilon_t^*\right)^2\right] \text{ when } \varepsilon_t > \varepsilon_t^* \end{cases} \tag{2}$$

where $\varepsilon_t^*(\sigma,T) = K_0 e^{cT}\sigma^m$; note that n, $A(T)$, m, K_0, c, $\Delta(\sigma)$ and $\delta(\sigma)$ are material parameters. A distinction is made between $\varepsilon_t < \varepsilon_t^*$ ("work hardening", $\dot{\varepsilon}_{vp} \to \dot{\varepsilon}_s$ "from above", $\dot{\varepsilon}_t > 0$) and $\varepsilon_t > \varepsilon_t^*$ ("recovery", $\dot{\varepsilon}_{vp} \to \dot{\varepsilon}_s$ "from below", $\dot{\varepsilon}_t < 0$). An example will be provided in Fig. 3. In terms of dislocation concepts, the transient responses reflect changes in the internal defect structure. Steady state (F = 1) corresponds to a dynamic equilibrium between work hardening and recovery. In the following, it is assumed that temperature is constant.

3. A test illustrating the "from below" and "from above" approaches

In Fig. 3, a σ_1 load is applied to a sample during a period of time [0, $t_{1\text{-}2}$], long enough for the internal parameter $\varepsilon_t(\sigma_1,t)$ to be close enough to its asymptotic value $\varepsilon_t^*(\sigma_1)$. At $t_{1\text{-}2}$, the applied load is increased from σ_1 to σ_2. Fast transient creep takes place and the internal parameter $\varepsilon_t(t)$ is rapidly larger than its asymptotic value associated with the initial load, $\varepsilon_t(\sigma_2,t) > \varepsilon_t^*(\sigma_1)$. At $t_{2\text{-}1}$, the applied load is decreased to its initial value σ_1. Now, $\varepsilon_t(\sigma_2,t) > \varepsilon_t^*(\sigma_1)$, and the internal parameter decreases to reach $\varepsilon_t^*(\sigma_1)$, ultimately.

In other words, the strain rate $\dot{\varepsilon}_{vp}\left(t\right)$ tends toward its steady state value $\varepsilon_s\left(\sigma_1\right)$ "from above" during the first phase of the test, and "from below" during the third phase. During such a test, both an upper and a lower bound of the steady state creep rate are obtained.

Such a test was first described by Wawersik and Preece.[2] During a creep test, a $\sigma_1 = 7\ \mathrm{MPa}$ load was applied during 150 days (phase 1); the strain rate at the end of this period was $\dot{\varepsilon} = 2.5\times10^{-10}\,\mathrm{s}^{-1}$. Stress control was lost during 56 hours: the applied stress increased to $\sigma_1 = 9\ \mathrm{MPa}$, approximately, (phase 2) before control was restored and the stress was set to $\sigma_1 = 7\ \mathrm{MPa}$ again (phase 3). During the two following months, the average strain rate remained consistently equal to $\dot{\varepsilon} = 5.6\times10^{-11}\,\mathrm{s}^{-1}$, smaller than what it was during phase 1.

4. Test performed on Landes salt

4.1. Testing device

It was said that, when trying to assess steady state strain rates at the laboratory, temperature fluctuations are a concern as they blur strain evolution. This is particularly true when, as in the test described in this paper, loads and strain rates are small. For this reason, the creep testing devices are installed in a dead-end gallery of a salt mine at Altaussee, Austria, where fluctuations of temperature and hygrometry (8.15 °C and 68% RH, respectively) are small ($\pm$ 0.01 °C and $\pm$ 0.5% RH, respectively).[4] Dead loads are applied. Sample diameter and height are ϕ = 70 mm and *h* = 140 mm, typically. During each test, four vertical displacement gages are used for redundancy; their resolution is $\delta h = 80$ nm (a strain of $\delta h/h = 8\times10^{-5}/140 \approx 6\times10^{-7}$). Displacements are recorded every minute.

4.2. Landes salt sample

A creep test was performed on a salt sample (see Fig. 4) from a Southwestern salt diapir in Landes, France. The sample was cored at a depth of 913 m. The sample is quite pure, having less than 5% (volume) of insoluble materials. Sample height and diameter are *h* = 130 mm and ϕ = 65 mm, respectively. It is known that, in the small stresses range, salt creep behavior is strongly dependent on grain size (inverse cubic dependency of the pressure-solution strain rate on grain size).[5] Average grain size of Landes salt was measured at Utrecht University, The Netherlands; its average value is $D = 5.6\ \mathrm{mm}$, with a standard deviation of $\Delta D = 2.8\ \mathrm{mm}$. It can be inferred that, when compared with other rock salts having greater grain sizes, Landes salt is likely to be creep-prone (at least for low applied stresses).

Landes salt (cored at the same depth) is currently being investigated at the laboratory-scale (at Mines ParisTech) by means of a testing campaign comprising confined short-term tests as well as confined long-term tests (with stress deviators in the range 3-21 MPa and temperatures from ambient to 70 ˚C). Results of these tests are analyzed using Lemaitre creep law[6] and a recently extended law.[7] The uniaxial formulation of Lemaitre creep law is

$$\dot{\varepsilon} = \dot{\gamma}_{vp} \quad \text{with} \quad d(\gamma_{vp}^{1/\alpha}) / dt = (\sigma / K(T))^{\beta/\alpha} \tag{3}$$

where α, β and $K(T) = K_r \exp\left(B\left(1/T - 1/T_{ref}\right)\right)$ are material parameters. Note that $\dot{\gamma}_{vp}$ is a strictly decreasing function (as $\alpha < 1$); in spite of including a small number of parameters, this law is able to describe a creep test during its full length. Note that from the analysis of the laboratory-scale results, $\alpha_{th} = 3\times10^{-5}\,/\,^{\circ}\mathrm{C}$.

4.3. Tests Results

4.3.1. Effects of the initial load

Low-stress creep tests began on October 8, 2018 at 10:30 am. The load initially applied was $\sigma_1 = 0.60$ MPa. Averaged values of the four strains measured every minute from October 8, 2018 to March 12, 2020 are shown in Fig. 5. Note that the curve is somewhat bumpy during the end of July 2019 – early August 2019 period, a phenomenon observed on most tests performed in the Altaussee mine during this period, probably due to an external event. The sample experiences a long transient period after which strain rates (computed with a 30-day span) are more or less stabilized.

At the end of this first period (October 27, 2019), strain rate was $\dot{\varepsilon} = 9\times10^{-12}\,\mathrm{s}^{-1}$. Two comments can be made. First, this rate (observed after 12 months) is faster than the strain rate extrapolated from high-stress creep tests ($\dot{\varepsilon} = 8.3\times10^{-15}\,\mathrm{s}^{-1}$ obtained with Lemaitre law, Eq. 3) by several orders of magnitude (note however that the lab tests and the Altaussee tests are not conducted under the same conditions). In addition, a creep test was performed on a second Landes salt sample. The applied stress was 0.2 MPa. After 12 months, the strain rate was $\dot{\varepsilon} = 3\times10^{-12}\,\mathrm{s}^{-1} \pm 1\times10^{-12}\,\mathrm{s}^{-1}$. This is not inconsistent with other tests performed in the mine in the same stress range which suggest that the strain rate versus stress relation might be linear[4]; laboratory tests on salt samples from a different location show a similar trend.[8] Second, it is faster than the strain rates previously observed (after 8 months) on Avery Island salt and Hauterives salt (whose grains are coarser) when the applied stress was 0.6 MPa.[4] These facts suggest that, rather than dislocation creep, a mechanism active at high stress, pressure solution creep, whose rate is a decreasing function of grain size, might be the main mechanism acting during this test.[4] A

consequence is that the explanation in terms of dislocation mechanisms which underlies Munson and Dawson[3] model (see Section 2) does not hold anymore. Pressure solution causes creep by mass transfer from grain boundaries under high normal stress to those under lower stress, a mechanism which implies very limited transient creep. Prof. Spiers from Utrecht University (personal communication) suggests that the transient creep observed during this test might be a combination of steadily decelerating transient creep due to dislocation processes, over-printed by a slow steady state creep rate due to pressure solution, which is gradually approached more and more closely; another possibility being that there are changes in the structure of grain boundaries due to pressure solution that could cause transient pressure solution behavior over several months. In fact, this question remains open to discussion; it must be mentioned that the strains are so small that detecting microstructural changes (e.g. grain shape changes) due to pressure solution is (still?) out of reach. In the following, it is accepted that Munson and Dawson mathematical model (Eq. 2) remains valid, whatever the underlying mechanisms are.

4.3.2. Effects of the load change

On October 28, 2019, at 7:52 am, the load was increased from $\sigma_1 = 0.60$ MPa to $\sigma_2 = 0.90$ MPa. Two days later, at 7:33 am, the load was decreased from $\sigma_2 = 0.90$ MPa to $\sigma_1 = 0.60$ MPa in an effort to mimic the kind of loading history applied by Wawersik and Preece.[2] Strain and temperature as a function of time are represented in Fig. 6. A dot is plotted every minute. From the picture, strain experiences fluctuations which are $\delta\varepsilon = \pm 0.6 \times 10^{-6}$, approximately, during the whole test, proving that average thermal fluctuations in the sample are $\delta T = \delta\varepsilon / \alpha_{th} = \pm 0.02°\mathrm{C}$ (note, however, that the sample is a less than perfect thermometer: it measures [through sample strain fluctuations] average sample temperature, rather than room temperature, as some delay is needed before the sample reaches thermal equilibrium with the gallery, see below). After the load increase, the strain rate experiences an abrupt increase and, two days later, it is $\dot{\varepsilon} = 8.3 \times 10^{-11}\mathrm{s}^{-1}$. Immediately after unloading (to $\sigma_1 = 0.6$ MPa), strain rate is negative (expansion) before increasing to $\dot{\varepsilon} = 4 \times 10^{-12}\mathrm{s}^{-1}$ after a couple of hours (it was $\dot{\varepsilon} = 9 \times 10^{-12}\mathrm{s}^{-1}$ before the load increase). Later on (Fig. 5) it stabilizes to $\dot{\varepsilon} = 5 \times 10^{-12}\mathrm{s}^{-1}$ after five months. This transient evolution can be explained, at least partly, by temperature changes and “reverse” creep.

Temperature fluctuations raise a difficult problem. In most cases, during load changes, temperature increases as people are working in the gallery, generating thermal expansion of the sample by $-\alpha_{th}\dot{T}$, and the actual strain rate is underestimated. Conversely, when staff leaves the gallery, temperature slowly (several days) decreases to reach equilibrium with the rock mass, and the

sample experiences thermal contraction. During this specific test, staff presence in the gallery was made as short as possible. However, during the load increase at 7:52 am on October 28, a temperature increase by $\delta T = 0.09°\mathrm{C}$ is clearly visible in Fig. 6; it generates a negative (expansion) strain which is smaller than $-\alpha_{th}\delta T = -2.7\times10^{-6}$. However, as a whole, room temperature fluctuations are smaller than 0.04 °C and fluctuations from thermal origin remain modest.

Removing the additional load $\delta\sigma = -0.30\ \mathrm{MPa}$ (-100 kg on a $\phi = 65\ \mathrm{mm}$ sample) on October 30 provides an opportunity to assess the elastic modulus. Removal is a relatively fast operation (a few seconds), performed somewhere between dot 1 and dot 2 (separated by one minute) in Fig. 6. Note that a one-minute long transformation is *adiabatic* (salt thermal diffusivity is around $k = 3\times10^{-6}$ m²/s and sample diameter is $\phi = 65\ \mathrm{mm}$; the characteristic time for thermal conduction in the salt cylinder is $\phi^2/k = 1400\ \mathrm{s}$). The strain change between 1 and 2 is $\delta\varepsilon = -1.12\times10^{-5}$. This strain change is the sum of an elastic and a viscoplastic strain change (likely to be small). It provides a lower bound for the elastic modulus, $E > \delta\sigma / \delta\varepsilon = 27\ \mathrm{GPa}$. Landes salt density is $\rho = 2150\ \mathrm{kg/m^3}$ and sound speed is $c = 3500$ m/s, from which an estimate of the *adiabatic* modulus is $E = \rho c^2 = 26.3$ GPa, in good agreement with what is observed during the load removal.

Negative (expansive) strain rates ("reverse creep") are typical of the effects of unloading and were observed during most tests in which unloading was managed.[9] Reverse creep is not taken into account in the model described by Eqs. 2 or 3, which must be adapted to account for reverse creep, for instance $\dot{\varepsilon}_s = A\sigma^n$ and $\sigma = B^{-1/p} - \dot{\varepsilon}_t\left|\dot{\varepsilon}_t\right|^{1/p-1} + \left(\varepsilon_t^*/K\right)^{1/m}$,where A, n, m, K and ε_t^* have the same meaning as in Eq. 2; B and p are two positive constants. In this model, reverse creep $(\dot{\varepsilon}_{vp} = \dot{\varepsilon}_t + \dot{\varepsilon}_s < 0)$ is observed until $\dot{\varepsilon}_t = -\dot{\varepsilon}_s$, see Fig. 7. Note that reverse creep has also been recently included in an extension of Lemaitre creep law.[10]

After several months, the strain rate stabilizes to $\dot{\varepsilon} = 5\times10^{-12}\mathrm{s}^{-1}$. Unfortunately, an electric outage occurred during two weeks, beginning November 19. It blurs the strain versus time curve at a critical period and it is difficult to assess precisely whether and when reverse creep comes to an end.

4.4. Upper bound and lower bound for steady state creep rate

These results suggest that both an upper bound and a lower bound of the steady state strain rate can be determined, provided that, during a creep test, the applied load is increased for some time before being restored. Strain rates before and after the load change (Fig. 8) provide an upper $(\dot{\varepsilon} = 9\times10^{-12}\mathrm{s}^{-1})$ and a lower bound ($\dot{\varepsilon} = 5\times10^{-12}\mathrm{s}^{-1}$), respectively. A condition, however, is that the

load increase be large and long enough (and the initial phase of the test be long enough) for the transient strain rate to become larger than its asymptotic value during the higher load phase, $\varepsilon_t(t_{2\to 1}) > \varepsilon_t^*(\sigma_1)$.

5. Conclusions and Perspectives

The creep test performed on a Landes salt sample confirms the results already obtained during an earlier testing campaign, supported by the Solution Mining Research Institute (SMRI), performed on Hauterives (France), Avery Island (Louisiana) and Gorleben (Germany) salt samples[4]: under uniaxial conditions, natural salt creeps even under very small loads suggesting that the stress threshold for the onset of creep is exceedingly small, or even zero. Even after one year, steady state is not reached, and the strain rate is faster than extrapolated from high-stress tests by several orders of magnitude. A second test (under a 0.2 MPa uniaxial load, not presented here) suggests that in the low stress range, the strain-rate versus stress relation is linear; this is also supported by previous creep tests performed at the laboratory-scale.[8]

In addition, a simple procedure (after one year, a larger load is applied during two days before coming back to the initial load) allows changing the sign of the strain rate, and the steady state strain rate is approached from above (before the load change) and from below (after the initial load is applied again). Both an upper bound and a lower bound are obtained for steady state creep rate. Depending on the stress deviator applied, the length of the first two phases can be adapted. For low applied stresses, temperature effects should be kept as small as possible for a correct interpretation of the test results. Reverse creep is observed: after unloading, the overall viscoplastic strain rate (not only the transient strain rate) changes sign.

Several questions remain open. First, the test was uniaxial, and one may ask whether the results would be changed if a confining pressure were applied in addition to the axial load. During an earlier campaign, a test was performed *on the same sample* both in the mine – in uniaxial conditions – and in RESPEC facilities at Rapid City – both in uniaxial and triaxial conditions (the applied deviatoric load was 3 MPa). No significant difference was found.[4] However, further research should be undertaken to assess the influence of the mean pressure on the time-dependent response of rock salt. Second, interpretation of the test makes use of a theoretical framework inspired by Munson and Dawson[3]: the viscoplastic strain rate can be split into a steady state part and a transient part. The transient part is such that, whatever sample past history, transient strain rate during a creep test (under a constant load) tends to a value which is a function of stress (and temperature) only. Challenging this fundamental assumption would require more and still longer tests. Finally, one may ask if these results make a change when the behavior of underground works is concerned. Generally speaking, the answer is positive, as suggested by several authors.[9,11-14] A definite proof could be

reached through field evidence. For instance, measuring brine outflow from a brine-filled cavern (which equals creep closure rate when thermal equilibrium has been reached[15]) before and after a cavern pressure drop would allow to confirm the notions explained in this Note. However, interpretation would not be easy as, in addition to rheological transient creep (as observed during laboratory tests), a cavern experiences “geometrical” transient creep closure that originates in the slow stress redistribution in the rock mass, a phenomenon which has no equivalent in a laboratory sample.

Acknowledgments

The authors are indebted to Dr. Suzanne Hangx and Caspar Sinn (PhD student) from Utrecht University, who kindly performed grain size analysis on Landes salt, and to Salinen Austria staff (Gerd Hofer and Stefan Simentschitsch) whose kind help has been instrumental. The authors benefited from Prof. Spiers' comments, also from Utrecht University, on the respective role of pressure solution and dislocation mechanisms during transient behavior under very low stresses. EDF, a French utility, kindly provided the salt samples. The testing facility at Altaussee, from which the present test benefited, was funded by the Solution Mining Research Institute, which also funded the test described in Fig. 1.

References

1. Bérest P, Gharbi H, Brouard B, Hofer G, Stimmisher S, Brückner D, DeVries K, Hévin G, Spiers CJ Uraï J, Bauer S (SMRI sponsor). *Very Slow Creep Tests As a Basis for Cavern Stability Analysis*, SMRI Research Report RR 2017-1;2017.
2. Wawersik WR, Preece DS. Creep Testing of Salt: Procedures, Problems and Suggestions. In: Hardy Jr. & Langer (Eds.), *Proceedings 1st Conference on the Mechanical Behaviour of Salt*, University Park, PA; 1984:421-449.
3. Munson DE, Dawson PR. Salt constitutive modelling using mechanism maps. In: Hardy Jr. & Langer (Eds.), *Proceedings 1st Conference on the Mechanical Behaviour of Salt*, University Park, PA; 1984:717-737.
4. Bérest P, Brouard B, Brückner D, DeVries K, Gharbi H, Hévin G, Hofer G, Spiers C, Uraï J. Very Slow Creep Tests on Salt Samples. *Rock Mech Rock Eng*. 2019;52:2917-2934. https://doi.org/10.1007/s00603-019-01778-9
5. Spiers CJ, Schutjens PMTM, Brzesowsky RH, Peach CJ, Liezenberg JL, Zwart HJ. Experimental determination of constitutive parameters governing creep of rocksalt by pressure solution. *Geological Soc., London, Special Publications*. 1990;54(1):215-227. https://doi.org/10.1144/GSL.SP.1990.054.01.21
6. Tijani M, Vouille G, Hugout B. Le sel gemme en tant que liquide visqueux. In: *5th International Congress on Rock Mechanics*, Melbourne, Australia; 1983:241–246.
7. Labaune P, Rouabhi A, Tijani M, Blanco-Martín L, You T. Dilatancy Criteria for Salt Cavern Design: A Comparison Between Stress- and Strain-Based Approaches. *Rock Mech Rock Eng*. 2018;51(2):599-611. https://doi.org/10.1007/s00603-017-1338-4
8. Tijani M, Hadj-Hassen F, Gatelier N. Improvement of Lemaitre's creep law to assess the salt mechanical behavior for a large range of deviatoric stress. In: Zuoliang (Ed.), *Proceedings 9th International Symposium on Salt*, Beijing; 2009:135-147.
9. Bérest P, Brouard B, Gharbi H. Rheological and geometrical reverse creep in salt caverns. In: Roberts, Mellegard, Hansen (Eds.), *Proceedings 8th Conference on the Mechanical Behaviour of Salt*, Rapid City, SD;2015:199-208.
10. Labaune P. *Comportement thermomécanique du sel gemme : application au dimensionnement des cavités*. Ph.D. thesis, MinesParisTech;2018.
11. Cornet JS, Dabrowski M, Schmid DW. Long-term cavity closure in non-linear rocks. *Geol J Int*. 2017;210(2):1231–1243. https://doi.org/10.1093/gji/ggx227
12. Marketos G, Spiers CJ, Govers R. Impact of rock salt creep law choice on subsidence calculations for hydrocarbon reservoirs overlain by evaporite caprocks. *J. Geophys. Res.: Solid Earth*. 2016;121(6):4249–4267.

https://agupubs.onlinelibrary.wiley.com/doi/abs/10.1002/2016JB012892

13. Van Sambeek LL, DiRienzo AL. Analytical solutions for stress distributions and creep closure around open holes or caverns using multilinear segmented creep laws. In: *Proceedings of SMRI Fall Meeting*, Salzburg;2016.
14. Bérest P, Manivannan S. Behavior of a salt cavern when creep law is modified to account for low deviatoric stresses. In: *Proceedings 53rd US Rock Mech/Geomech Symp*, New York;2019:Paper 19-477.
15. Brouard B, Bérest P, de Greef V, Béraud JF, Lheur C, Hertz, E. Creep closure rate of a shallow salt cavern at Gellenoncourt, France. *Int J Rock Mech Min Sci*. 2013;62:42-50. https://doi.org/10.1016/j.ijrmms.2012.12.030

List of figures

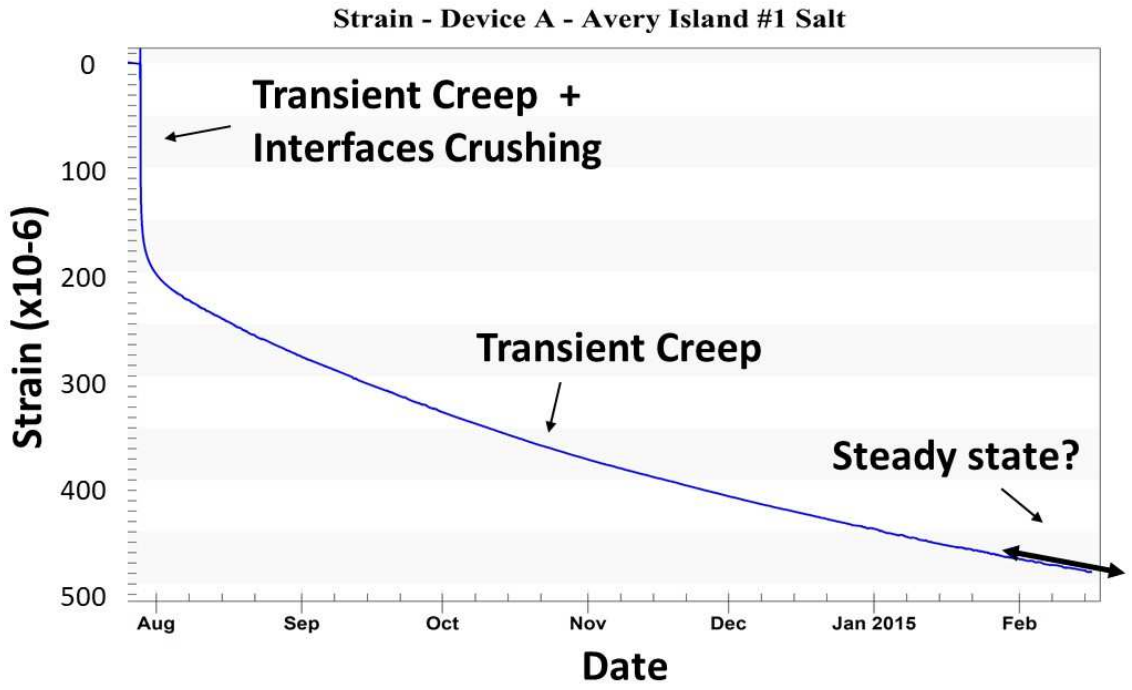

(b)

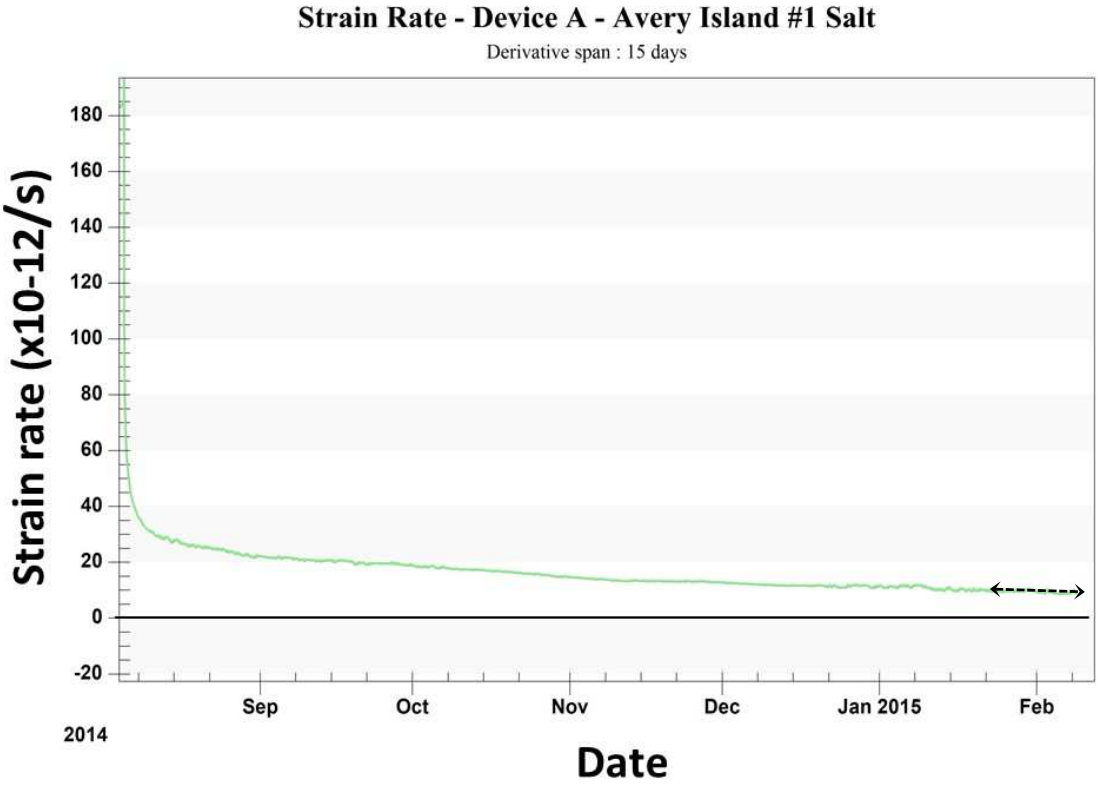

Figure 1. Strain (a) and strain rate (b) as a function of time during a uniaxial creep test on an Avery Island salt sample. Sample height is 140 mm, with a slenderness ratio of 2. The axial load is $\sigma = 0.2$ MPa. Strains are measured every minute.[1]

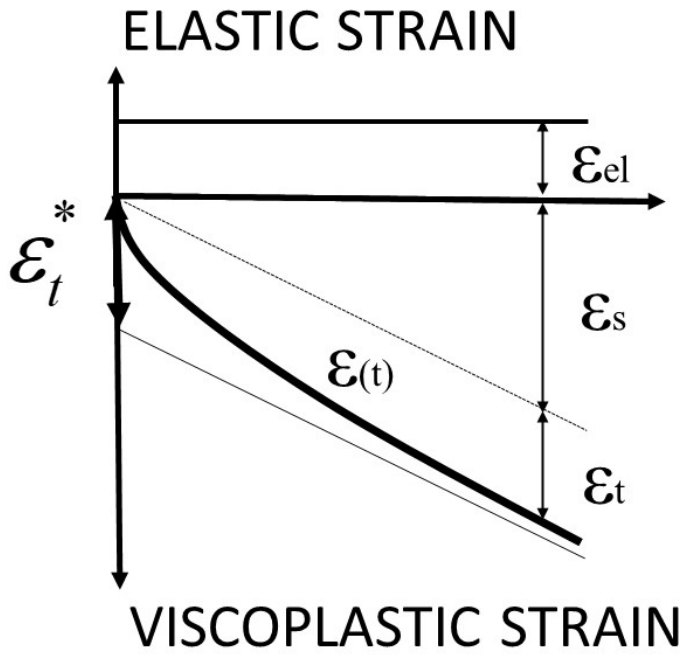

Figure 1. Schematic description of a creep test (the applied load, σ, is constant).

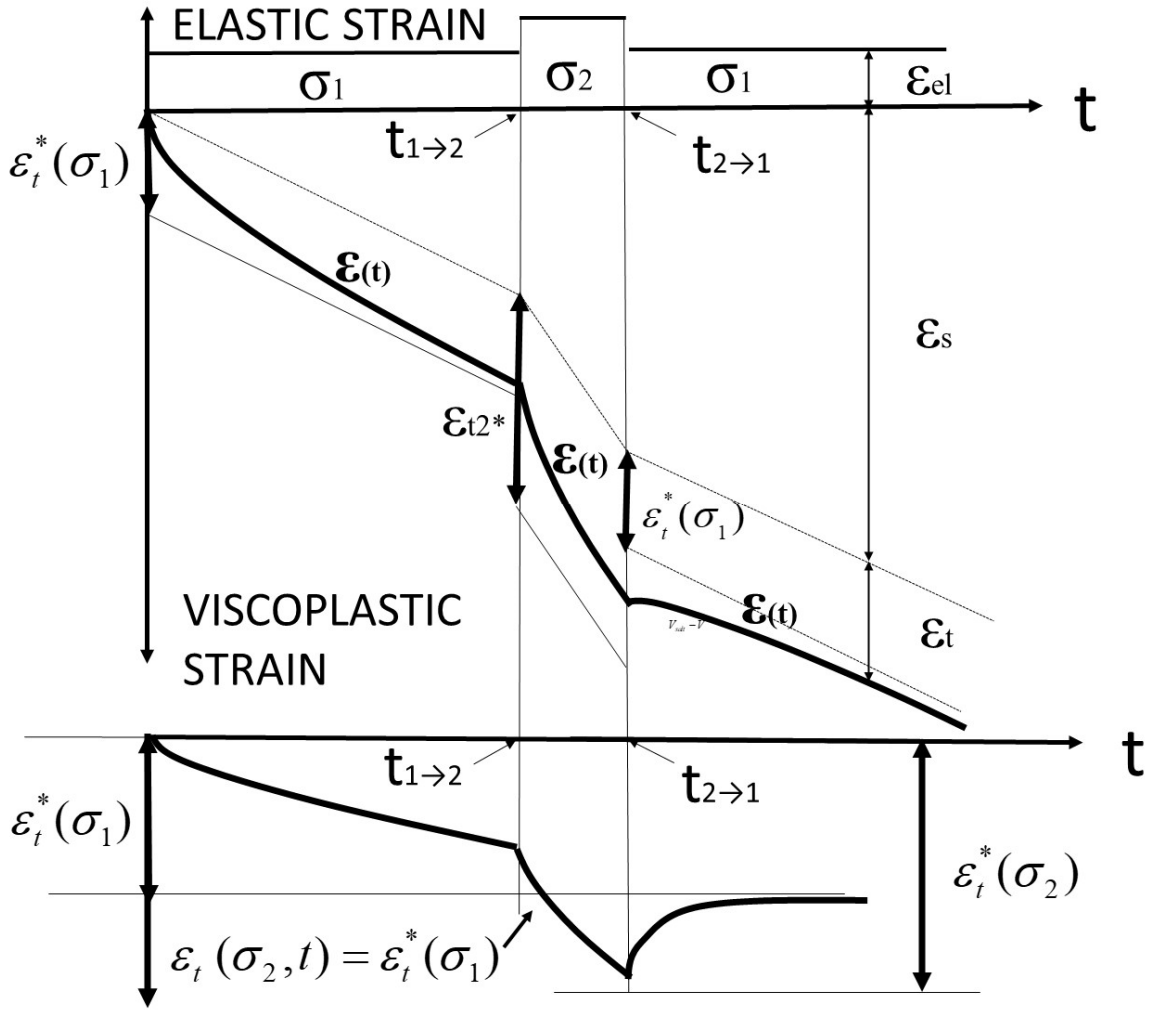

Figure 1. A creep test including a stress step from σ_1 to σ_2 followed by a step from σ_2 to σ_1.

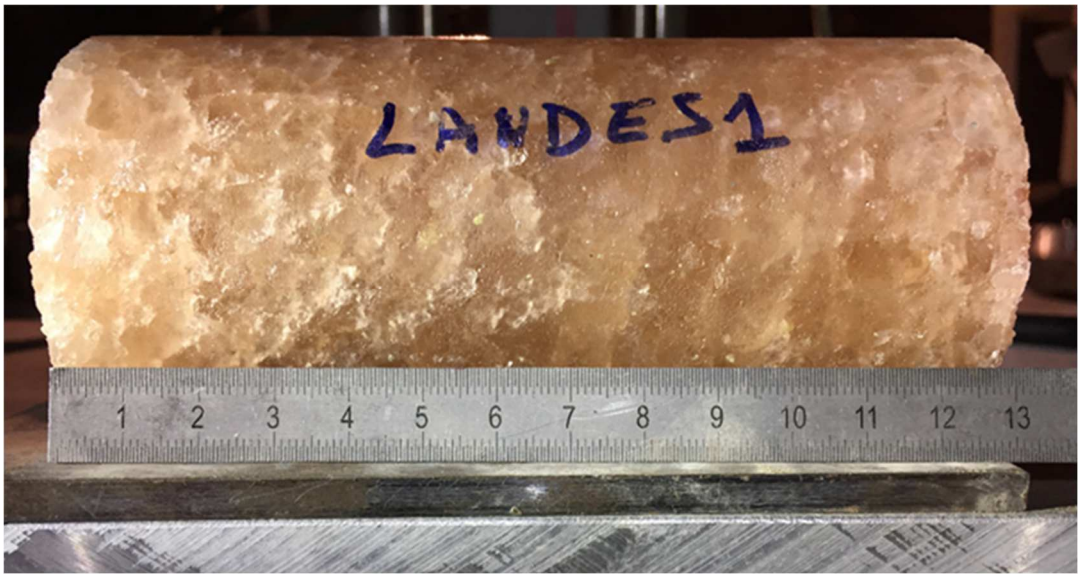

Figure 1. View of Landes 1 sample before testing.

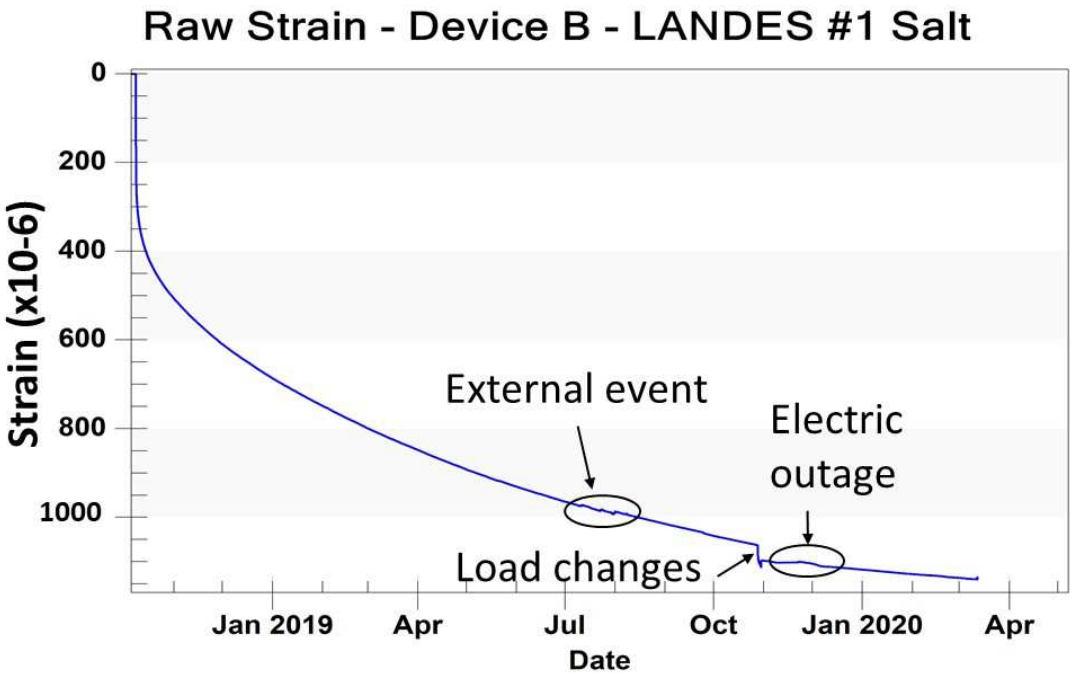

Figure 1. Average strain as a function of time from October 8, 2018 to March 12, 2020.

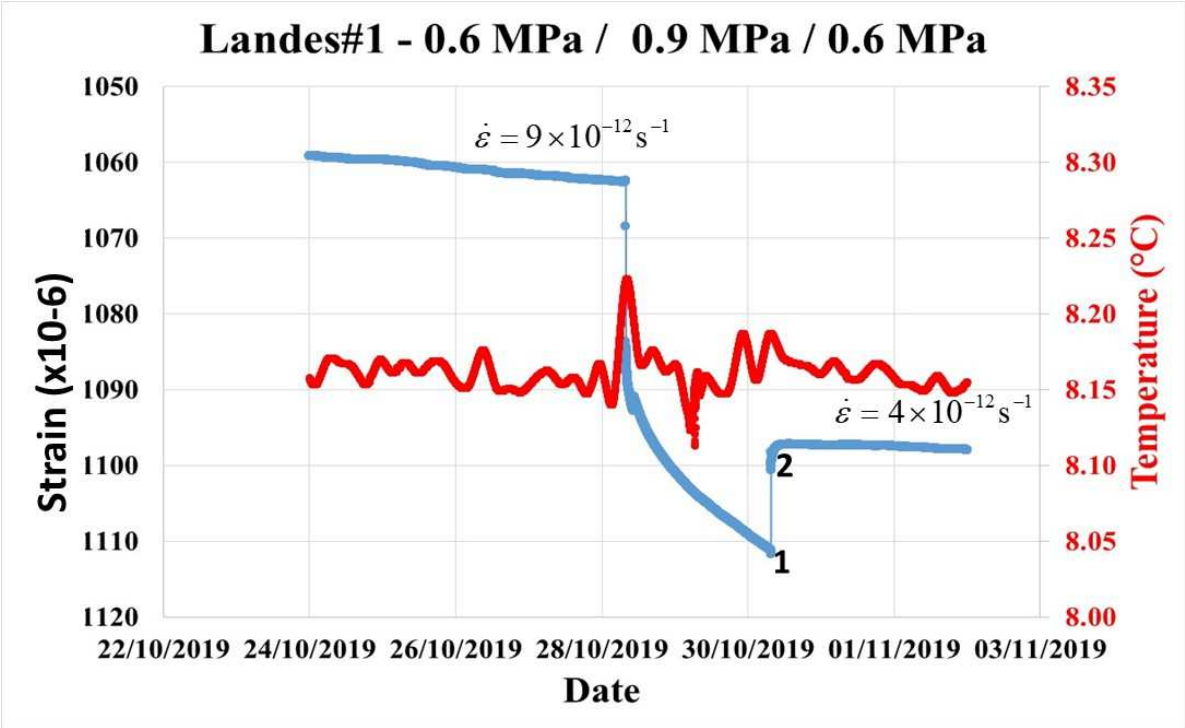

Figure 1. Strain and Temperature (measured every minute) as a function of time during the load changes.

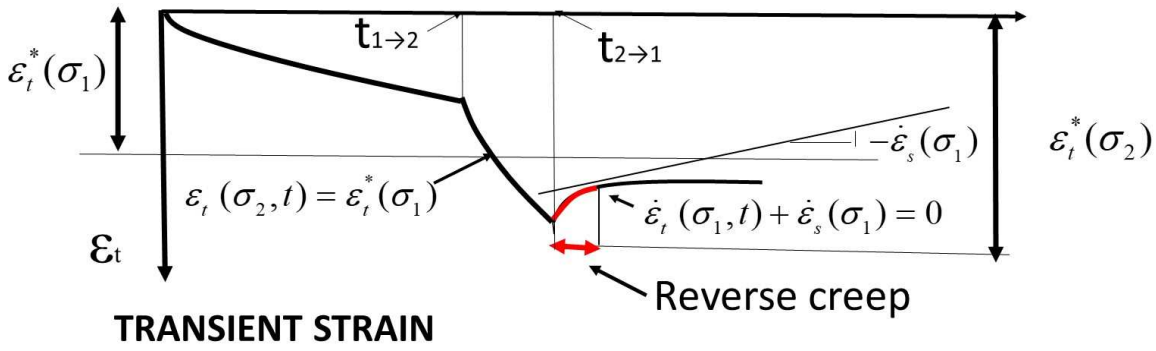

Figure 1. Transient creep and reverse creep.

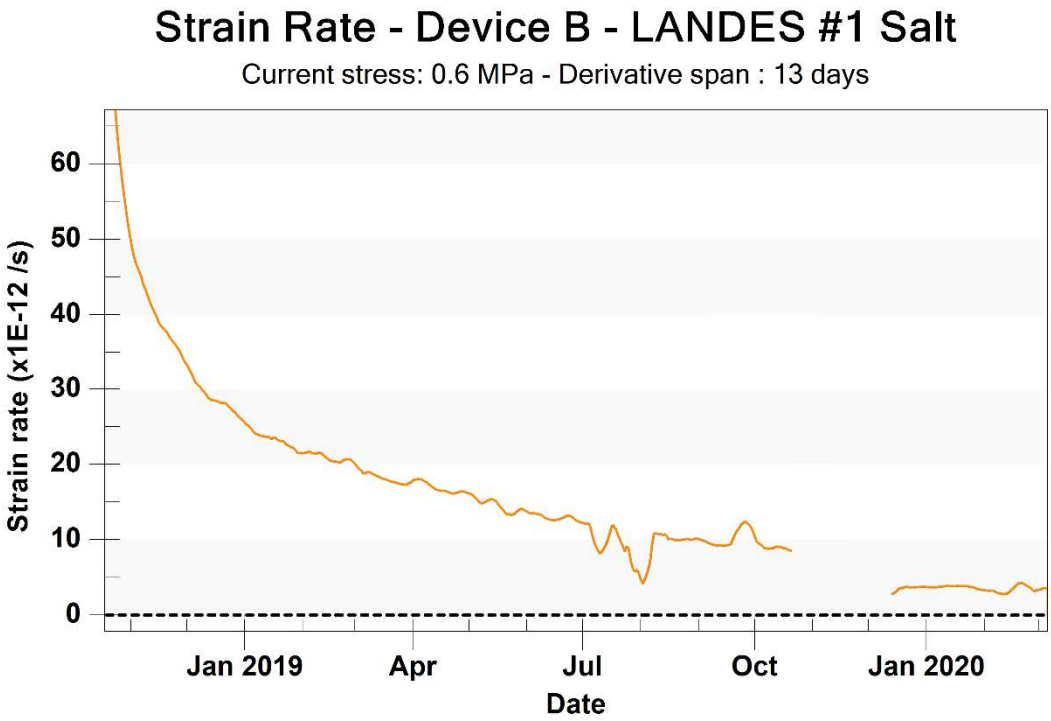

Figure 1. Computed strain rates with a time span of 13 days (selecting this span implies that strain rates 13 days before, 13 days after and during the load change cannot be represented).